

Pyramidal Arborizations and Activity Spread in Neocortex

Adrian Robert

Department of Cognitive Science, 0515 University of California, San Diego; La Jolla, CA 92093-0515, USA; arobert@cogsci.ucsd.edu

Abstract

A model of a patch of neocortex was constructed by reference to the details of pyramidal and inhibitory arbors in rat somatosensory cortex, and its behavior was compared to slice experiments measuring activity spread following point-stimulation. Two features of pyramidal arbors played a prominent role in the results and may affect cortical information transmission: 1) dual horizontal structure, in which connections are made densely within 0.5 mm and sparsely over 2-3 mm – affected characteristic length and rate of propagation; 2) significant restriction of projections to the vertical compartment (superficial, middle, deep) of origin – resulted in laminar differences in activity levels.

Key words: Neocortex; Lamination; Propagation

1 Introduction

Each hemisphere of the neocortex consists of a relatively flat, laminated sheet in which several anatomically distinguishable layers (six, by convention) of cells are juxtaposed. In addition to local connections, cells within one localized region, or *area*, project to and receive from a limited set of other areas. These projections originate from and terminate in subsets of the layers, often following particular patterns [3] (fig. 1, left). During sensory processing, they convey stimulus-related activity from essentially one starting point (the “primary area”) through a network of areas (about 30 in the visual system of macaque monkeys and higher primates). Usually, connections from areas synaptically closer to the primary area to those further away follow the FF pattern, while those in the opposite direction follow the FB pattern (fig. 1, left). Presumably these patterns reflect a computational need to treat stimulus-driven activity differently from internal state-driven activity in each area [10], however it is difficult to make this more precise simply based on the anatomy, because most cortical celltypes possess dendritic and axonal arborizations extending over multiple layers [6] (fig. 1, right). On the other hand, technical constraints

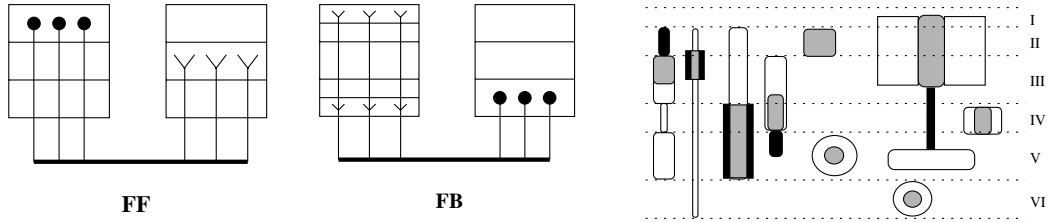


Fig. 1. As noted in [3], connections between areas fall largely into one of the two forms on the left; FF and FB stand for ‘feedforward’ and ‘feedback’ respectively. The right figure illustrates typical within-area cortical cell arborization patterns. Black, white, and grey indicate dendritic, axonal, and overlapping arborizations.

render it difficult to physiologically determine the quantitative impacts that different inputs have on areas.

We have therefore taken an approach via modeling, constructing a series of three models incorporating differing levels of anatomical detail. The most complex model contained six layers and could be compared directly with simple physiological experiments for purposes of verification and calibration. The simplest contained a single layer, and was best suited for theoretical analysis and comparison with a number of previous cortical models. The third model was intermediate in complexity, containing three layers, and represented a compromise affording both comparison with physiology and investigation of computational properties. In this note we describe the construction of the models and the comparison of the 3- and 1-layer versions with experimental results on spread of activity in rat somatosensory neocortical slices. The results highlight and quantitatively characterize important basic aspects of the horizontal and vertical connections underlying cortical information transfer.

2 Model Construction

All three models shared the same basic structure: a stack of square grids of cell units interconnected with strengths decaying exponentially over horizontal distance. The whole represented a 2x4 mm patch of neocortex, simulating 1 in 30 cells. The main goal guiding construction was accurate representation of aspects of the biology most likely to affect interlayer information transmission. Because the amount of time for transfer between layers can determine dynamical structure such as local feedback circuits that could magnify or shrink influences, a single cell model capable of representing this temporal element was chosen. Because the arborization characteristics of the different celltypes determine routes of interlayer communication, the distribution and arborization of the different celltypes (fig. 1) was used to determine connectivity.

2.1 *Cell Unit*

Cortical cells were modeled by single compartment conductance-based units analogous to those described in [13]. Membrane potential is updated every 10^{-4} sec according to synaptic and leak current across a capacitive membrane. If the membrane potential reaches threshold in a unit, it is reset to the resting potential and a spike is propagated with a delay to synapses on other cells, the effects of which are modeled by alpha-function conductance changes. The time constants and peak conductances for synapses were determined according to what portion of the cell the particular class of input involved is known from anatomical data to contact. Cortical cells fall into three classes based on intrinsic response properties [9]. Additional conducting channels were included in the cell models to mimic the effects of currents differentiating these classes. See [12] for further detail.

2.2 *Six-Layer Model*

The 6-layer model was an attempt to be maximally faithful to what is known about the structure of rat sensory cortex and served as a basis for simplification to build the other models. It was constructed in 3 stages – first, anatomical data on cells and their interconnections was gathered by surveying the literature. This resulted, after some initial simplification, in 51 separate cell populations, consisting of 14 pyramidal populations (75% of the total cells) plus 11 subtypes of inhibitory cells split into several populations each. The relative numbers of each population and their interconnections are not fully specified by the literature, however the values that are known constrain the others. We therefore made educated estimates of unknown qualities and then adjusted all values by means of a relaxation network.

In this network, each cell population was represented by a single node with a density value and a set of values representing outputs to other nodes. On each optimization step, these latter values were propagated to their targets scaled by relative densities to set input values, which were then compared with known or estimated values to compute error. This error was applied to adjust the outputs and densities based on the relative confidences in estimated values. Simulated annealing was employed to relax the network, and, while different runs led to different sets of final values, any particular value would vary no more than 10%, suggesting that the baseline estimated value set was situated within a broad, flat minimum in the space of architectures.

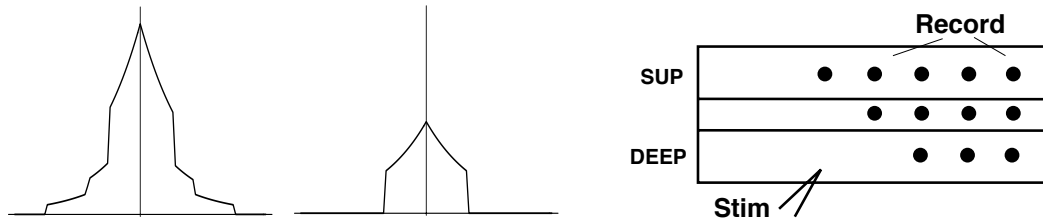


Fig. 2. Left: typical pyramidal influence via axonal arbor on same compartment (left) and both other compartments combined (right); to scale, arbitrary units (the within-compartment shape results from superposition of 3 arbor widths with different frequencies of occurrence – typically 0.5, 1, and 2 mm in the rat). Right: Schematic of the experimental setup.

2.3 Three-Layer Model

We constructed the 3-layer model based on insights from building the 6-layer one. Regarding pyramidal cells, axon tracing studies in rat SI and elsewhere [5,8] show that their arborizations possess three general characteristics (see fig. 2, left):

- In a given layer, some cells give rise to wide arbors stretching over distances of more than a millimeter, while other cells have narrower arbors of much less than a millimeter range.
- Terminal distribution remains largely (usually $\sim 70\%$) within the compartment of the the cell soma – either superficial (layers I–III), middle (layer IV), or deep (layers V–VI).
- The widest portions of arbors from cells in a layer remain within the same compartment.

Based on this, the three layers in the simpler model represented these three compartments, with a single pyramidal population in each arborizing as described. Regarding inhibitory cells, a reduction in number of types from 11 to 3 was achieved by collapsing highly similar ones. The first class consists of small inhibitory cells with axons and dendrites localized within a compartment (e.g., neurogliaform, chandelier), the second consists of wide inhibitory cells also largely localized within a compartment (e.g., large basket), while the third consists of narrow inhibitory cells with arbors spanning compartments (e.g., bipolar). In the model, the middle layer contained only the first type, while the other two contained all three, leading to a total of just 10 cell populations including 3 pyramidal.

2.4 Single Layer Model

The 1-layer model contained two cell populations (excitatory and inhibitory) and was constructed by computing average horizontal arborizations for cell classes in the 6-layer model. To investigate the composite structure of pyramidal arbors horizontally (fig. 2, left), four versions of this model were constructed. In the “baseline”

condition, these arbors were directly modeled by a weighted sum-of-exponentials. In the “short condition”, only the shortest exponential, renormalized, was used. In the “average” condition, a single exponential out to the weighted average maximum radius of the arbors was used, while in the “fit” condition, a single exponential arbor was least-squares fit to the weighted average. Each of these lateral connectivity conditions led to differences in activity propagation, to be described.

3 Experimental Comparison

All three models were compared to two sets of experiments on cortical slices measuring activity spread following point stimulation at the layer VI-white matter boundary [1,7]. Previously [11], we reported comparisons involving the 1-layer and 6-layer models, showing that they, like the slices, displayed three regimes of quiescence, wave propagation, and explosion depending on the relative strengths of inhibitory synapses. Additionally the 6-layer model captured certain aspects of the first experiment that the single-layer model did not. Here, we discuss these aspects and others in greater detail for the 3-layer model, whose behavior was qualitatively similar to that of the 6-layer one, focusing on the effects of the characteristics of pyramidal arborizations discussed above.

3.1 Horizontal Activity Spread

Figure 2 (right) depicts the experimental setup in both [1] (henceforth, CC) and [7] (LS). The pharmacological conditions and methods of measurement were slightly different in the two cases, but they both observed propagation of waves of activity at a certain rate and width, reproduced in all three models [11].

LS also observed that activity appeared to propagate in discrete steps: the first wave of synaptically-stimulated activity following stimulation was observable only out to about 200-300 μm on either side; the time to earliest activity further out was greater by an amount consistent with (increasingly) multisynaptic transmission. LS interpreted this as indicating that pyramidal-pyramidal connections are sufficiently strong to support large-scale activity transmission only within a range of $<400 \mu\text{m}$. Figure 3 shows similar results from three versions of the 1-layer model illustrating the effects of pyramidal horizontal arbor structure.

Note that, in addition to variation in transmission distance, differences in wavelength and speed are also visible. The “short” condition, not shown, was similar to the baseline except that, due to the lack of longer-distance arbors, propagation was from 20-50% slower depending on disinhibition level.

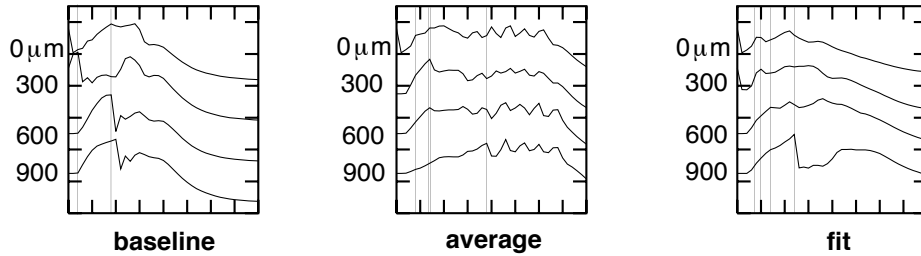


Fig. 3. Variation in monosynaptic transmission distance with model connectivity. Each of the three plots displays membrane potential over 40 msec for cells at successively further points from the origin (top trace). The vertical lines indicate the first peaks of the traces; in each case, there is a jump from peaks being within < 5 msec of each other (a shorter time than required for charging and synaptic transmission) to being much further apart. For the baseline case, this occurs between 300 and 600 μm , for the average and fit cases, between 600 and 1200 μm .

3.2 Vertical Transfer

CC and LS recorded from both deep and superficial cortex, finding indication that activity spread preferentially through the deep layers. CC found while recording intracellularly from superficial pyramidal cells that during extracellular field potential events accompanying wave passage, the cells often did not fire, and in fact even displayed depressed membrane potentials relative to rest. On the other hand, they found that deep pyramidal cells, particularly burst cells, almost always fired. LS found activity appeared to travel faster in the deep layers – in particular, a delay of almost 9 msec between the earliest deep and earliest superficial activities occurred at 1.5 mm lateral distance.

The 3-layer model showed similar behavior (fig. 4). Intuitively, activity is initially strongest in the deep layers owing to the proximity of the stimulation site and, aided by partial isolation, continues to propagate there more strongly. Comparison (not shown) with noncompartmentalized versions of the model, in which pyramidal connections were made equally throughout all layers, supported this explanation, because the latter versions did not display any interlayer differences in activity after the first few milliseconds.

4 Computational Implications

Many models have investigated Hebbian development of connection weights to single, laterally-connected cortical layers exposed to input with correlation structure [2], but these generally only take into account the shortest excitatory lateral interactions – corresponding to the “short” condition here. The prominence of the longer connections in determining propagation rate and other characteristics of activity

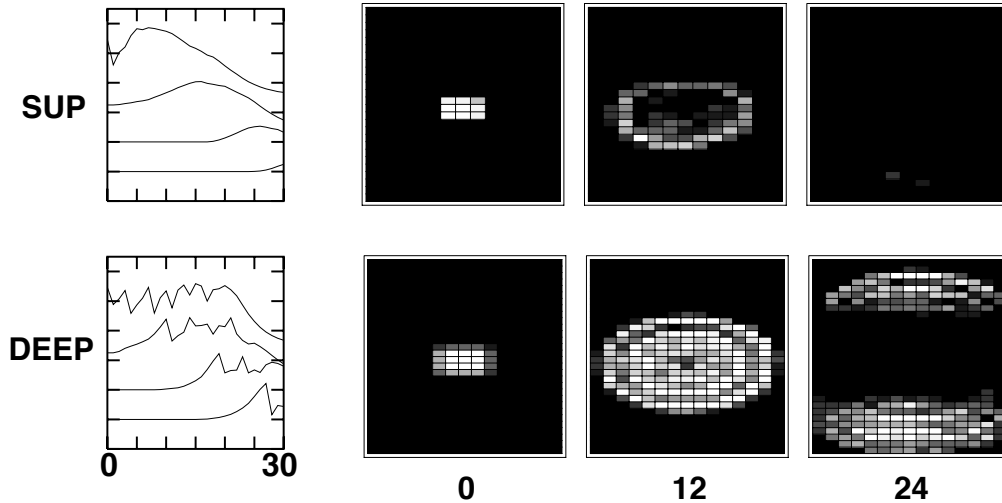


Fig. 4. Wave propagation activity in superficial and deep layers in 3-layer model. Left: membrane potential traces as in figure 3 for 4 locations over 30 msec. Right: spiking activity of all the pyramidal cells in each layer for three successive times (msec) – each point is the firing rate averaged locally over 4x4 cells and 2 msec (lighter = more active). Deep activity propagates further, faster, and with greater amplitude. (The middle layer was intermediate.)

waves in our anatomically-based models suggests that they should be included as well; theoretical analyses [4] emphasize that lateral length constants are important.

Comparatively few cortical models [10] have incorporated laminar structure, largely because the relevant architectural details are not clear from the biology. The present work suggests based on convergent evidence that processing with different compartments is partially independent, and it lays foundations for investigating this quantitatively. The 3-layer model is currently being employed to study Hebbian learning under the influence of feedforward and feedback inputs. Although this model was based on rat primary sensory cortex, a preliminary survey of data on areas in other regions and species suggests that at its level of detail, the situation is fairly similar across other areas and other species.

Biosketch

Adrian Robert received Bachelor's degrees in computer science and mathematics from Cornell University in 1992. He went on to study in the cognitive science department at the University of California at San Diego, where he is now finishing up his doctoral thesis on computational aspects of the medium-scale anatomical structure of the mammalian cerebral cortex.

References

- [1] Y. Chagnac-Amitai and B.W. Connors. Horizontal spread of synchronized activity in neocortex and its control by GABA-mediated inhibition. *J. Neurophysiol.* **61** (1989) 747–58.
- [2] E. Erwin, K. Obermayer, and K. Schulten. Models of orientation and ocular dominance columns in the visual cortex: A critical comparison. *Neural Computation* **7** (1995) 425–68.
- [3] D.J. Felleman and D.C. Van Essen. Distributed hierarchical processing in the primate cerebral cortex. *Cerebral Cortex* **1** (1991) 1–47.
- [4] G.J. Goodhill. The influence of neural activity and intracortical connections on the periodicity of ocular dominance stripes. *Network* **9** (1998) 419–32.
- [5] J.P. Gottlieb and A. Keller. Intrinsic circuitry and physiological properties of pyramidal neurons in rat barrel cortex. *Exper. Brain Res.* **115** (1997) 47–60.
- [6] E.G. Jones and A. Peters, editors. *Cerebral Cortex, Vol. I. Cellular Components of the Cerebral Cortex*. (Plenum, New York, 1984).
- [7] R.B. Langdon and M. Sur. Components of field potentials evoked by white matter stimulation in isolated slices of primary visual cortex: Spatial distributions and synaptic order. *J. Neurophysiol.* **64** (1990) 1484–1501.
- [8] J.B. Levitt, D.A. Lewis, T. Yoshioka, and J.S. Lund. Topography of pyramidal neuron intrinsic connections in macaque monkey prefrontal cortex (areas 9 and 46). *J. Comp. Neurol.* **338** (1993) 360–76.
- [9] D.A. Prince and J.R. Huguenard. Functional properties of neocortical neurons. In W. Singer and P. Rakic, editors, *Neurobiology of Neocortex* (Wiley, New York, 1988).
- [10] R.P.N. Rao and D.H. Ballard. Dynamic model of visual recognition predicts neural response properties in the visual cortex. *Neural Computation* **9** (1997) 805–47.
- [11] A. Robert. A model of the effects of lamination and celltype specialization in the neocortex. In J.M. Bower, editor, *Computational Neuroscience: Trends in Research, 1998* (Plenum, New York, 1998).
- [12] A. Robert. Lamination and activity spread in mammalian neocortex: A model. *J. Neurosci.* (submitted, 1998).
- [13] M.A. Wilson and J.M. Bower. The simulation of large-scale neural networks. In C. Koch and I. Segev, editors, *Methods in Neuronal Modeling* (MIT Press, Cambridge, Mass., 1989).